GAMMA-RAY BURSTS DETECTED BY *INTEGRAL*

L. Hanlon[1], S. Foley[1], S. McBreen[2], S. McGlynn[1], and B. McBreen[1]

[1] *School of Physics, University College Dublin, Dublin 4, Ireland*
[2] *Max-Planck-Institut für extraterrestrische Physik, 85748 Garching, Germany*

ABSTRACT

INTEGRAL has detected and localised 37 long-duration Gamma-Ray Bursts (GRBs) in the period from October 2002 to July 2006. We discuss the global characteristics of this GRB sample, using data obtained from the imager, IBIS, and spectrometer, SPI, on board *INTEGRAL*. Spectral, spatial and temporal characteristics of the prompt gamma-ray emission are presented for a selection of the GRBs. *INTEGRAL*'s capabilities for the measurement of GRB spectral lag and polarisation are also discussed.

Key words: gamma-rays – bursts.

1. INTRODUCTION

The INTEGRAL Burst Alert System (IBAS) [1] is an automatic ground-based system for the accurate localisation of GRBs and the rapid distribution of GRB coordinates, providing, on average, 0.8 GRBs per month with an error radius of ∼3 arcminutes. *INTEGRAL* [2] has detected 37 long-duration GRBs since its launch in October 2002, including the low-luminosity GRB 031203 [3, 4], the weak X–ray rich GRB 040223 [5] and the very intense burst GRB 041219a [6]. There are two main γ-ray instruments on board, namely IBIS [7] and SPI [8], optimised for high-resolution imaging and spectroscopy, respectively, of the γ-ray sky. These are supported by an optical camera (OMC) and X–ray monitor (JEM-X). Independent spectroscopic redshifts have been determined for three *INTEGRAL* GRBs – GRB 031203 at z=0.1055 [9], GRB 050502a at z=3.793 [10] and GRB 050525a at z=0.606 [11].

The spatial distribution, in galactic coordinates, of the GRBs observed in the fully and partially coded field of view (16°×16°) of IBIS is shown in Fig. 1. The distribution is concentrated toward the Galactic plane, reflecting the direction in which the satellite is pointed for the majority of its exposure time. Fig. 2 compares the peak flux distribution of the GRBs observed by IBIS on *INTEGRAL* from October 2002 and July 2006 to the peak flux distribution of the

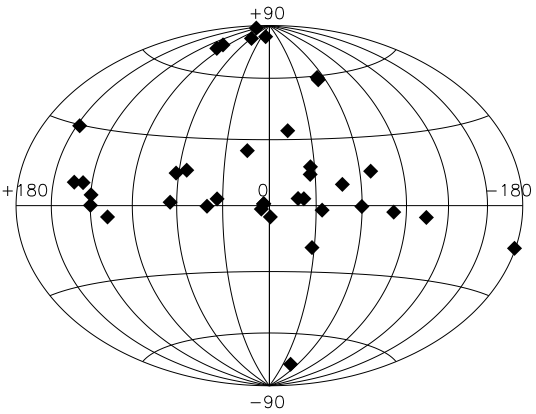

Figure 1. Spatial distribution in galactic coordinates of INTEGRAL GRBs from October 2002 to July 2006.

GRBs detected by the BAT instrument on *Swift* [12] from November 2004 to July 2006. It can be seen from Fig. 2 that *INTEGRAL* detects a higher fraction of weak GRBs than *Swift*.

2. GRBS DETECTED WITH SPI'S ANTI-COINCIDENCE SHIELD

The Anti-Coincidence Shield (ACS) of the SPI instrument works as a highly-sensitive GRB detector above ∼ 80 keV but lacks spatial and spectral information [13]. The ACS consists of 91 BGO crystals with a total mass of 512 kg surrounding SPI. It has a maximum sensitivity to GRBs at ∼ 90 ° from the satellite pointing direction and provides lightcurves in 50 ms bins with limited directional information provided by the shielding of SPI. The ACS detects GRBs at a rate of ∼1 every 2–3 days. A selection of GRBs detected with SPI-ACS is shown in Fig. 3. Temporal analysis of a more complete sample is presented in [14].

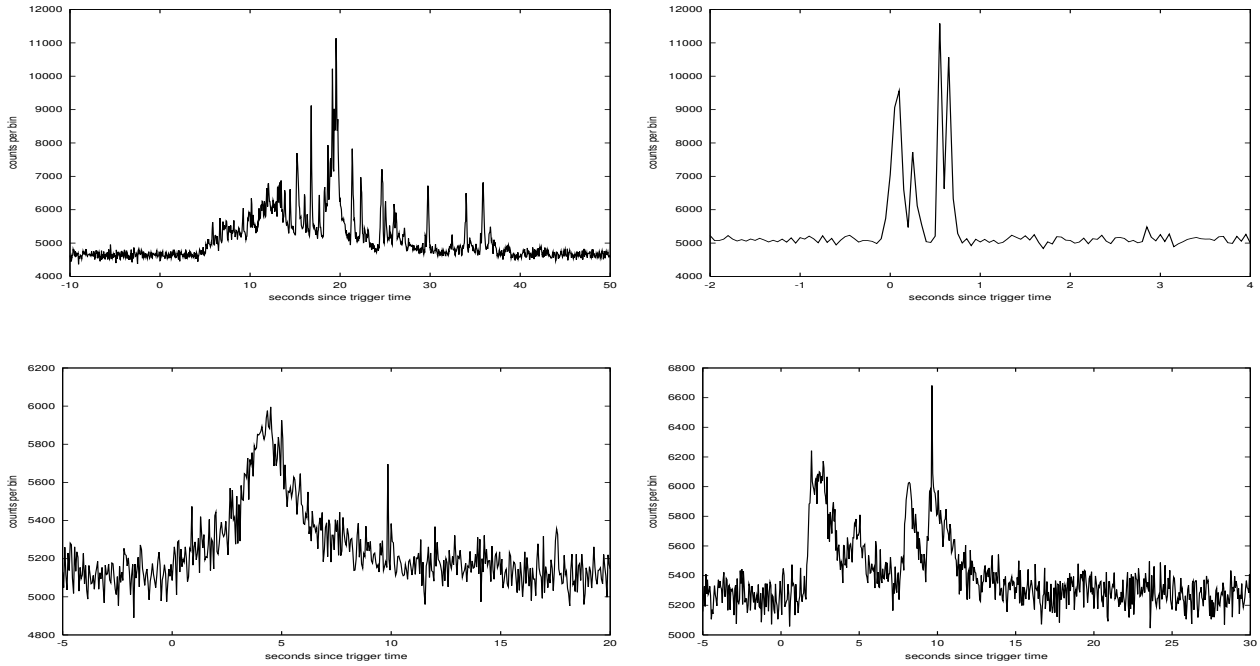

Figure 3. A selection of GRB lightcurves detected by the Anti-Coincidence Shield at energies > 80 keV.

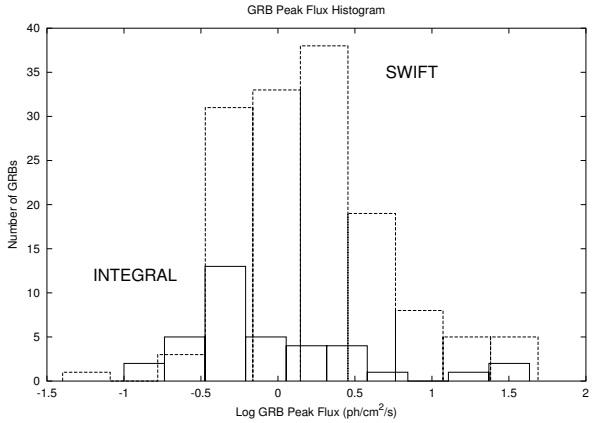

Figure 2. Peak flux distribution for GRBs detected by INTEGRAL from October 2002 to July 2006 (solid line) and Swift from November 2004 to July 2006 (dashed line).

3. GRBS IN THE FIELD OF VIEW OF SPI AND IBIS

The temporal and spectral properties of the GRBs detected by *INTEGRAL* from October 2002 to July 2006 are given in Table 1. Limited spectral information is available for GRB 021125 due to significant telemetry loss while the satellite was in calibration mode. Data for GRB 050918 and GRB 050922a are not yet publicly available and information is taken from Götz et al. [15] and Götz et al. [16], respectively. Durations are obtained from the IBAS notifications. Peak flux values given are integrated over a 1 second time interval in the 20–200 keV energy band. Fluences are also measured over 20–200 keV. Photon indices are for a power-law fit to the spectra in the 20–200 keV energy range. Spectral parameters for those spectra for which the Band model [17] is fit are given in Table 2. GRB 041219a is the exception, with peak flux, fluence and spectral parameters measured with SPI in the 20 keV–8 MeV energy range. Some of the more notable *INTEGRAL* bursts are now discussed in more detail.

Table 2. GRBs for which a Band Model is fit to spectra. Parameters quoted are low-energy power-law index, α, high-energy power-law index, β, and break energy, E_0. † indicates β is fixed at this value.

GRB	α	β	E_0 [keV]
GRB 030131	1.4 ± 0.2	3.0 ± 1.0	70 ± 20
GRB 040422	1.26 ± 0.08	$4^\dagger$	56 ± 17
GRB 041218	1.14 ± 0.20	2.08 ± 0.16	80 ± 40
GRB 041219a	1.43 ± 0.08	2.06 ± 0.12	299.2 ± 76.2
GRB 050502a	0.89 ± 0.25	$3^\dagger$	84 ± 44
GRB 050520	1.45 ± 0.21	$3^\dagger$	266 ± 1847
GRB 050525a	0.99 ± 0.12	$3^\dagger$	55 ± 35

*Table 1. Temporal and Spectral Properties of GRBs detected by INTEGRAL up to July 2006. The columns refer to (from left to right): GRB; right ascension; declination; duration; peak flux (20–200 keV); fluence (20–200 keV); photon index of power-law fit to spectrum; afterglow detections in radio, R, infrared, IR, optical, O and X–ray, X. RA, DEC and duration values taken from http://ibas.iasf-milano.inaf.it/IBAS_Results.html. GRBs for which information is unavailable are denoted by *.*

GRB	RA	DEC	Duration [s]	Peak Flux $erg\,cm^{-2}\,s^{-1}$	Fluence $erg\,cm^{-2}$	Photon Index, α ($\frac{dF}{dE} \propto E^{-\alpha}$)	Afterglow
GRB 021125 [30]	19:47:57	28:23:35	25	*	*	*	–
GRB 021219 [31]	18:50:27	31:57:17	5.5	3.5×10^{-7}	9.0×10^{-7}	2.00 ± 0.10	–
GRB 030131 [32]	13:28:21	30:40:43	124	1.7×10^{-7}	7.0×10^{-6}	Table 2	O
GRB 030227 [33]	04:57:34	20:28:16	33	9.6×10^{-8}	7.5×10^{-7}	1.85 ± 0.20	O,X
GRB 030320 [34]	17:51:36	-25:18:52	48	5.4×10^{-7}	1.1×10^{-5}	1.69 ± 0.08	–
GRB 030501 [35]	19:05:33	06:15:57	40	2.5×10^{-7}	3.0×10^{-6}	1.75 ± 0.10	–
GRB 030529	09:40:30	-56:20:31	20	3.7×10^{-8}	4.0×10^{-7}	1.71 ± 0.20	–
GRB 031203[a] [3]	08:02:32	-39:50:47	39	2.5×10^{-7}	2.0×10^{-6}	1.63 ± 0.06	R,O,X
GRB 040106 [36]	11:52:18	-46:47:15	47	6.5×10^{-8}	8.2×10^{-7}	1.72 ± 0.15	O,X
GRB 040223 [5]	16:39:31	-41:55:47	258	1.6×10^{-8}	4.4×10^{-7}	2.30 ± 0.20	X
GRB 040323	13:53:49	-52:20:45	14	2.0×10^{-7}	3.0×10^{-6}	1.44 ± 0.18	O?
GRB 040403 [37]	07:40:54	68:12:55	21	4.3×10^{-8}	5.0×10^{-7}	1.90 ± 0.15	–
GRB 040422 [38]	18:42:01	01:59:04	10	1.8×10^{-7}	3.4×10^{-7}	Table 2	O
GRB 040624 [25]	13:00:08	-03:34:08	35	4.0×10^{-8}	1.0×10^{-6}	2.10 ± 0.20	–
GRB 040730	15:53:14	-56:28:15	43	3.4×10^{-8}	6.6×10^{-7}	1.44 ± 0.14	–
GRB 040812	16:26:05	-44:42:32	19	5.0×10^{-8}	2.3×10^{-7}	2.34 ± 0.29	O?,X
GRB 040827	15:17:00	-16:08:21	49	6.0×10^{-8}	1.2×10^{-6}	1.83 ± 0.18	O,X
GRB 040903	18:03:22	-25:15:23	10	2.0×10^{-8}	1.1×10^{-7}	3.08 ± 0.46	–
GRB 041015	00:18:37	66:51:37	30	4.0×10^{-8}	7.0×10^{-7}	1.28 ± 0.24	–
GRB 041218	01:39:06	71:20:05	60	2.8×10^{-7}	5.5×10^{-6}	Table 2	O
GRB 041219a [6]	00:24:26	62:50:06	350	1.84×10^{-5}	5.7×10^{-4}	Table 2	R,O
GRB 050129	16:51:12	-03:04:44	20	3.0×10^{-8}	4.5×10^{-7}	2.03 ± 0.38	–
GRB 050223	18:05:36	-62:28:26	50	6.0×10^{-8}	8.5×10^{-7}	1.84 ± 0.30	X
GRB 050502a[b]	13:29:45	42:40:27	20	2.0×10^{-7}	1.4×10^{-6}	Table 2	IR,O
GRB 050504	13:24:00	40:41:45	80	6.0×10^{-8}	1.4×10^{-6}	1.31 ± 0.10	X
GRB 050520	12:50:03	30:27:02	80	5.0×10^{-8}	1.8×10^{-8}	Table 2	X
GRB 050522	13:20:35	24:47:30	15	2.2×10^{-8}	9.0×10^{-8}	3.11 ± 0.58	X?
GRB 050525a[c]	18:32:33	26:20:23	12	3.2×10^{-6}	6.6×10^{-6}	Table 2	O,X
GRB 050626	12:26:58	-63:08:03	60	2.0×10^{-8}	8.7×10^{-7}	2.24 ± 0.15	–
GRB 050714a	02:54:21	69:07:34	40	1.5×10^{-8}	5.0×10^{-7}	2.13 ± 0.19	O?,X
GRB 050918	17:50:26	-25:24:51	130	8×10^{-8}	2×10^{-6}	*	X
GRB 050922a	18:04:37	-32:01:24	25	*	1×10^{-7}	*	X
GRB 051105b	00:37:51	-40:28:52	20	3.0×10^{-8}	2.9×10^{-7}	1.97 ± 0.24	–
GRB 051211b	23:02:45	55:04:44	80	6.1×10^{-8}	2.0×10^{-6}	1.72 ± 0.12	O,X
GRB 060114	13:01:07	-04:44:53	100	3.0×10^{-8}	1.3×10^{-6}	1.20 ± 0.19	–
GRB 060130	15:16:54	-36:54:43	40	2.0×10^{-8}	3.0×10^{-7}	1.81 ± 0.37	–
GRB 060204a	15:28:56	-39:26:38	78	2.1×10^{-8}	6.6×10^{-7}	1.63 ± 0.28	–

[a] $z = 0.1055$
[b] $z = 3.793$
[c] $z = 0.606$

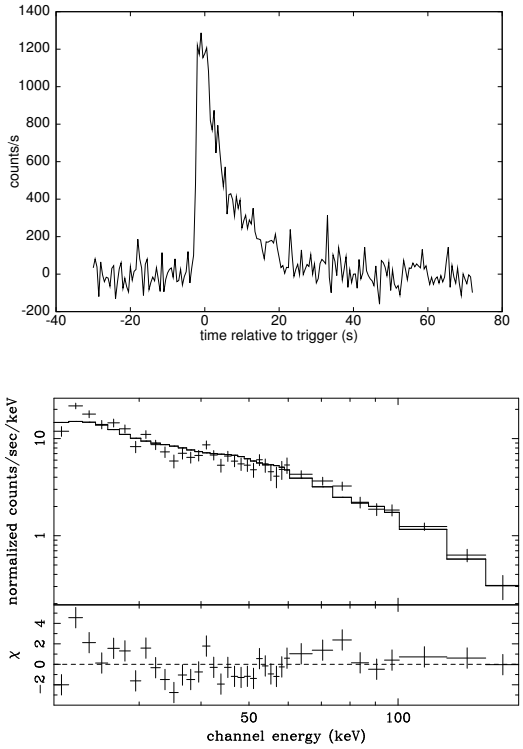

Figure 4. **a)** *IBIS lightcurve of GRB 031203 in the energy range 20–200 keV.* **b)** *IBIS spectrum of GRB 031203 from ∼20–200 keV fit with a power law of spectral index* -1.63 ± 0.06.

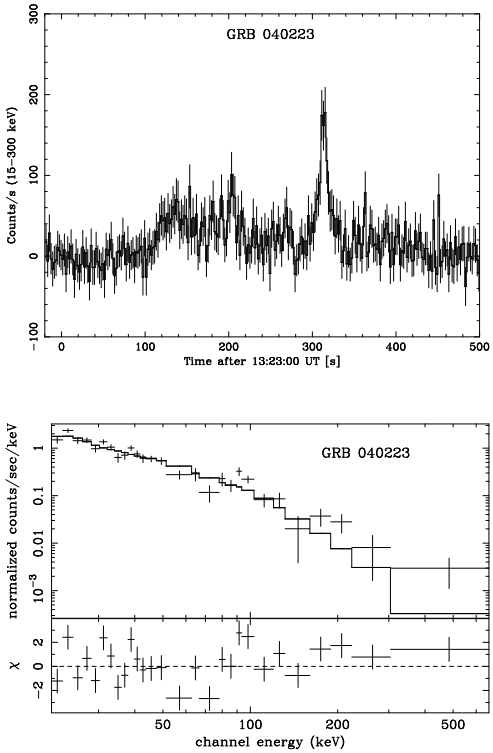

Figure 5. **a)** *IBIS lightcurve of GRB 040223 in the energy range 20–200 keV.* **b)** *IBIS spectrum of the main pulse of GRB 040223 over ∼20–200 keV, fit with a power law.*

3.1. GRB 031203

GRB 031203 is the third nearest GRB detected to date at $z = 0.1055$ [9] and is notable for its unambiguous association with the supernova SN2003lw [18]. The lightcurve shown in Fig. 4(a) exhibits a single-peaked structure with a duration of ∼30 seconds. Fig. 4(b) shows the spectrum of the burst which is well-fit by a power-law with a spectral index of -1.63 ± 0.06. It has a peak flux of 2.5×10^{-7} ergs cm^{-2} s^{-1} and a fluence of 2×10^{-6} ergs cm^{-2} [3]. The IBAS localisation of GRB 031203 enabled XMM-Newton to begin follow-up observations 6 hours later. The X–ray observations showed concentric ring-like structures centred on the GRB location, making this the first ever detection of a GRB X–ray "halo", caused by X–ray scattering from dust columns along the line of sight to the GRB [19]. A very high soft X–ray flux was inferred implying that this GRB was in fact an X–ray Flash (XRF) [4]. However, this interpretation is hard to reconcile with the hard IBIS spectrum.

3.2. GRB 040223

GRB 040223 was localised by IBAS and observed by XMM-Newton 5 hours after the burst trigger. The IBIS light curve is shown in Fig. 5(a) and includes two weak emission pulses before the main pulse, which result in the long duration of 258 s given in Table 1. Fig. 5(b) shows the spectrum of the main pulse of GRB 040223, with a peak flux of $(1.60 \pm 0.13) \times 10^{-8}$ ergs cm^{-2} s^{-1}, a fluence of $(4.4 \pm 0.4) \times 10^{-7}$ ergs cm^{-2} and a steep photon power law index of -2.3 ± 0.2, in the energy range 20–200 keV [5]. The steep spectrum implies it is an X–ray rich GRB with emission up to 200 keV and $E_{\rm peak} < 20$ keV.

3.3. GRB 041219a

GRB 041219a is the brightest burst to be localised by *INTEGRAL* [6]. The peak flux of 43 ph cm^{-2} s^{-1} (20 keV–8 MeV, 1 s integration) is greater than that of ∼98% of all BATSE bursts and the total duration of ∼350 s is longer than all but a small number of bursts. The lightcurve, shown in Fig. 6(a), exhibits a multi-peaked structure, with a precursor of ∼7 s duration, followed by a period of quiescence lasting ∼200 s. The most intense emission occurred about ∼250 s after the precursor, enabling optical and near infrared telescopes to observe the emission simultaneously. Fig. 6(b) shows the spectrum of the entire GRB which is well fit by the Band model with parameters given in Table 2.

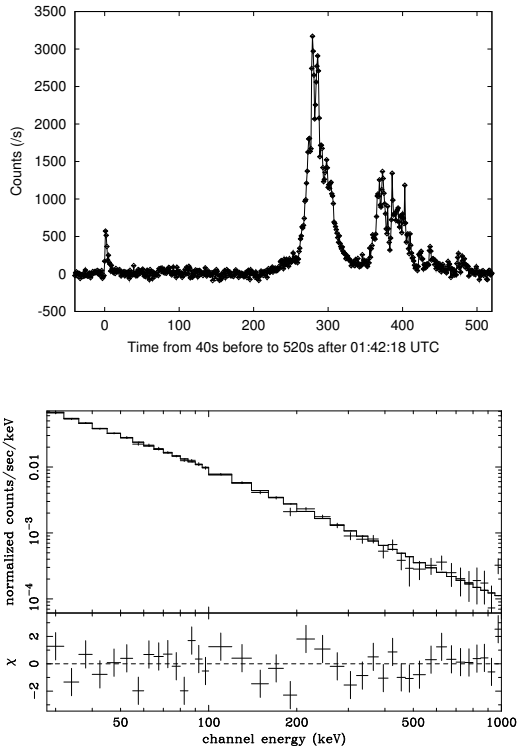

Figure 6. **a)** *SPI lightcurve of GRB 041219a in the energy range 20 keV–8 MeV.* **b)** *SPI spectrum of GRB 041219a from ∼20 keV–1 MeV fit by a Band model.*

4. POLARISATION ANALYSIS OF GRB 041219A

The SPI instrument may be used to measure GRB polarisation through multiple scattering events in its 19 Ge detectors [20], since the scatter angle depends on the polarisation of the incoming photon [21]. A search for linear polarisation in the most intense pulse (66 seconds) of GRB 041219a was performed in the 100–350 keV and 100–500 keV energy ranges. The multiple event data from the spectrometer was analysed and compared with the predicted instrument response obtained from Monte–Carlo simulations using the GEANT 4 mass model. The azimuthal scattering angle distribution was compiled and the degree of polarisation may be calculated from the modulation amplitude of this distribution. Results of this analysis indicate a high level of polarisation, but at a low level of significance, consistent with independent analyses [23]. Detailed results will be presented elsewhere [22].

5. X–RAY RICH GRBS DETECTED BY *INTEGRAL*

X–ray flashes, X–ray rich GRBs and classical GRBs appear to possess a continuum of spectral properties and it is probable that they have a similar origin [24]. *INTEGRAL* has detected a number of X–ray rich GRBs, including the X–ray flashes XRF 040903 and XRF 050522. As can be seen from Table 1 many of the *INTEGRAL* GRBs have steep power-law spectra, indicating that their break energies are below the range of the *INTEGRAL* instruments, i.e., < 20 keV. There is therefore an excess of counts in the X–ray/low γ-ray region, implying that they are X–ray rich. These bursts tend to be weak and their time profiles consist of long, slow pulses. Examples include GRB 040223, GRB 040624, GRB 050626 and GRB 060130 (Fig. 7).

6. DARK GRBS DETECTED WITH *INTEGRAL*

Almost 60% of the GRBs observed by *INTEGRAL* do not have a detected optical afterglow. This may be due to a number of factors, including dust obscuration along the line of sight to the GRB, an intrinsically faint afterglow, a rapidly decaying afterglow or the burst occurring at high redshift. *INTEGRAL* also points preferentially towards the Galactic plane, and therefore tends to select bursts whose afterglow emission is heavily obscured at optical wavelengths. However, a separate population of intrinsically "dark" GRBs may exist with a very faint or undetectable optical afterglow.

GRB 040223 and GRB 040624 (Fig. 7) provide good examples of a population of GRBs with dark or faint optical afterglows [25]. GRB 040223 was observed close to the Galactic plane, so NIR observations were carried out to overcome the high dust obscuration. Observations were undertaken at the NTT of ESO, 17 hours after the GRB and no afterglow was found. GRB 040624 was located far from the Galactic plane at high latitude where the optical extinction is negligible. Afterglow observations were carried out 13 hours after the burst using the VLT and TNG. Magnitude limits were obtained in the optical that are fainter than the very faint end of the distribution of the magnitudes of a compilation of 39 promptly observed counterparts.

7. SPECTRAL LAGS

It is an observed property of GRBs that lower energy γ-ray emission lags higher energy emission, producing a time delay between low and high energy GRB

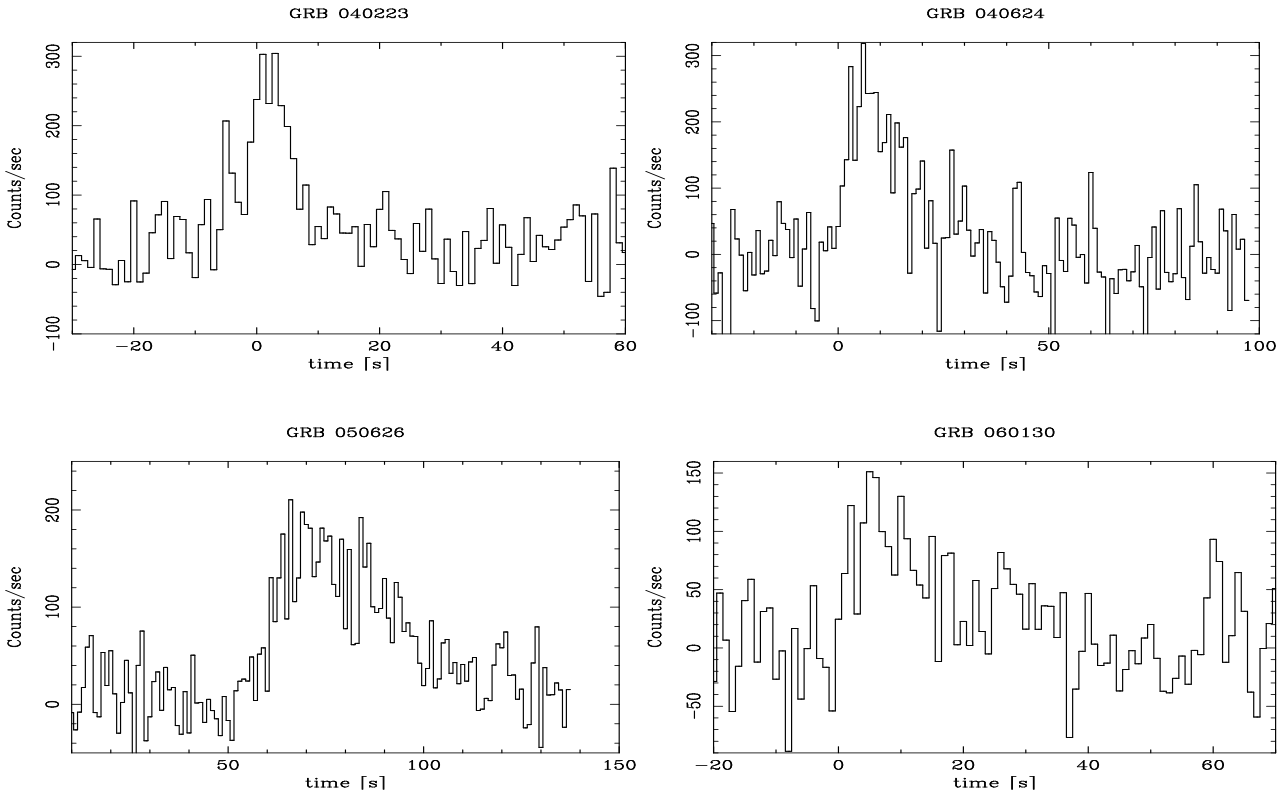

Figure 7. Examples of weak, X-ray rich GRB IBIS lightcurves with photon indices >2 (1s resolution, 25–300 keV).

lightcurves. This time lag can be determined by computing the cross-correlation function (CCF) between the two time profiles. The peak of this function then corresponds to the spectral lag of the GRB. A significant correlation has been found between spectral lag and isotropic luminosity for GRBs [26]. The spectral lag of a GRB can therefore be used, in principle, as a distance indicator, based solely on its prompt γ-ray emission.

Fig. 8 shows the IBIS time profile of GRB 031203 in the 25–50 keV and 50–300 keV energy bands and the corresponding cross-correlation function (CCF). A third order polynomial is fit to the CCF and the peak of the fit is taken to be the spectral lag. This analysis yields a spectral lag of 0.17 ± 0.05 s for GRB 031203, consistent with previous lag results for this GRB ([3],[27]). GRB 031203 has a peak luminosity of $\sim 7 \times 10^{48}$ ergs cm^{-2} s^{-1}, causing it to fall below the lag–luminosity correlation [28], as does the other notable low-luminosity burst, GRB 980425.

A spectral lag of 4.85 ± 0.30 s was measured for GRB 040827 (Fig. 9). GRB 040827 has a peak flux of 6×10^{-8} ergs cm^{-2} s^{-1} and a steep photon index of 1.83 ± 0.18, making it one of a number of weak, X-ray rich GRBs with long spectral lags.

The spectral lag distribution of a number of *INTEGRAL* GRBs as a function of their peak flux is shown in Fig. 10. Preliminary analysis suggests that weak GRBs with low peak flux tend to have the longest spectral lags [29]. The lag-luminosity relationship implies that these long-lag weak GRBs have inherently low luminosities.

8. DISCUSSION

INTEGRAL observations of gamma-ray bursts have yielded many interesting results and offer significant insight into the prompt γ-ray emission. IBAS successfully provides accurate, fast localisations of GRBs to the community at a rate of ~ 0.8 GRB per month, enabling multi-wavelength afterglow observations to be carried out by other space-based missions and ground-based telescopes. Polarisation measurements are being carried out using *INTEGRAL*'s SPI instrument using its array of 19 hexagonal Ge detectors. The IBIS instrument allows for the analysis of multi-band lightcurves in order to determine the spectral lags (and hence luminosities) of the observed bursts. *Swift* detects more GRBs due to its larger field of view. *INTEGRAL*, however, detects proportionally more weak and X–ray rich GRBs.

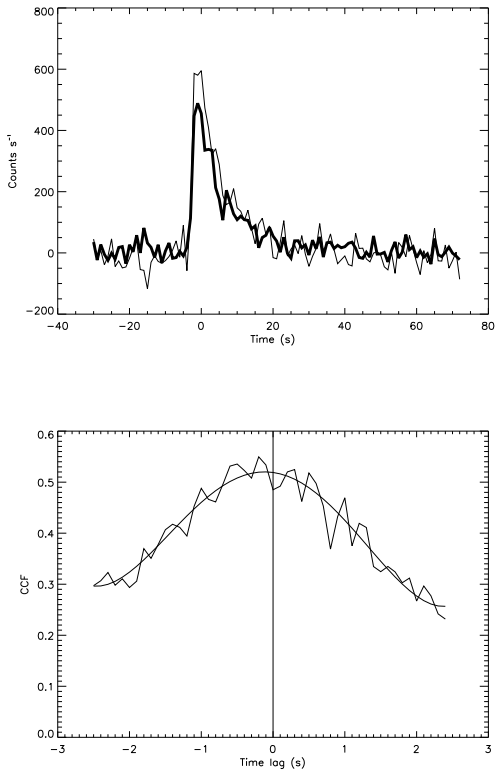

Figure 8. **a)** *IBIS lightcurve of GRB 031203 in the energy ranges 25–50 keV (dark line) and 50–300 keV (light line).* **b)** *CCF of GRB 031203 indicating a lag of* 0.17 ± 0.05 *s. The vertical line represents the point of zero lag.*

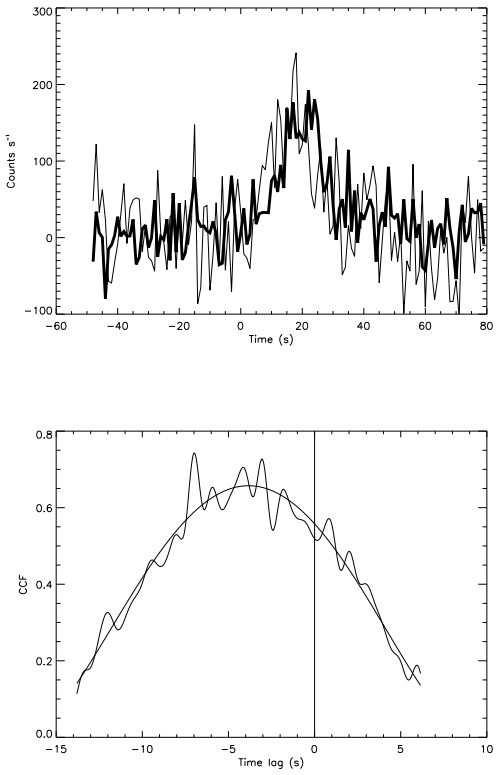

Figure 9. **a)** *IBIS lightcurve of GRB 040827 in the energy ranges 25–50 keV (dark line) and 50–300 keV (light line).* **b)** *CCF of GRB 040827 indicating a lag of* 4.85 ± 0.30 *s. The vertical line represents the point of zero lag.*

REFERENCES

[1] Mereghetti S., Götz D., Borkowski J., et al., 2003, A&A 411, L291

[2] Winkler C., Courvoisier T. J. L., Di Cocco G., et al., 2003, A&A 411, L1

[3] Sazonov S. Yu., Lutovinov A. A. & Sunyaev R. A., 2004, Nature 430, 646

[4] Watson D., Hjorth J., Levan A., et al., 2004, ApJ 605, L101

[5] McGlynn S., McBreen S., Hanlon L., et al., 2005, Il Nuovo Cimento 28, 481

[6] McBreen S., Hanlon L., McGlynn S., et al., 2006, A&A 455, 433

[7] Ubertini P., Leburn F., Di Cocco G., et al., 2003, A&A 411, L131

[8] Vedrenne G., Roques J. P., Schönfelder V., et al., 2003, A&A 411, L63

[9] Prochaska J. X., Bloom J. S., Chen H. -W., et al., 2004, ApJ 611, 200

[10] Prochaska J. X., Ellison S., Foley R. J., et al., GCN 3332

[11] Foley R. J., Chen H. -W., Bloom J., et al., GCN 3483

[12] Gehrels N., Chincarini G., Giommi P., et al., 2004, ApJ 611, 1005

[13] von Kienlin A., Beckmann V., Rau A., et al,. 2003, A&A 411, L299

[14] Rau A., von Kienlin A., Hurley K., et al., 2005, A&A 438, 1175

[15] Götz D., Mereghetti S., Shaw S., et al., 2006, GCN 4002

[16] Götz D., Mereghetti S., Shaw S., et al., 2006, GCN 4007

[17] Band D., Matteson J., Ford L., et al., 1993, ApJ 413, 281

[18] Malesani D., Tagliaferri G, Chincarini C., et al., 2004, ApJ 609, L5

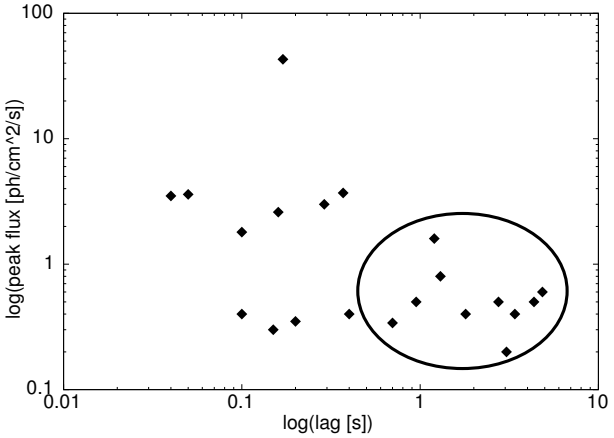

Figure 10. Spectral lag distribution of INTEGRAL GRBs as a function of peak flux (20–200 keV). GRBs with the longest lags (circled region) tend to have low peak fluxes.

[19] Vaughan S., Willingale R., O' Brien P. T., et al., 2004, ApJ 603, L5

[20] Kalemci E., Boggs S., Wunderer C., et al., 5th *INTEGRAL* Workshop 2004

[21] Lei F., Dean A.J., & Hills G.L., 1997, Sp. Sci. Rev. 82, 309

[22] McGlynn S., Clark D. J., Dean A. J., et al., submitted to A&A

[23] Kalemci E., Boggs S., Kouveliotou C., et al., 2006, astro-ph/0610771

[24] Sakamoto T., Lamb D. Q., Graziani C., et al., 2004, ApJ 602, 875

[25] Filliatre P., Covino S., D'Avanzo P., et al., 2006, A&A 448, 971

[26] Norris J. P., 2002, ApJ 579, 386

[27] Shrader C. R., 2006, AIPC 836 185

[28] Gehrels N., Norris J. P., Mangano V., et al., 2006, astro-ph/0610635

[29] Foley S., et al. in prep.

[30] Malaguti G., Bazzano A., Beckmann V., et al., 2003, A&A 411, L307

[31] Mereghetti S., Götz D., Beckmann V., et al., 2003, A&A 411, L311

[32] Götz D., Mereghetti S., Hurley K., et al., 2003, A&A 409, 831

[33] Mereghetti S., Götz D., Tiengo A., et al., 2003 ApJ 590, L73

[34] von Kienlin A., Beckmann V., Covino S., et al., 2003, A&A 411, L321

[35] Beckmann V., Borkowski J., Courvoisier T.J., et al., 2003, A&A 411, L327

[36] Moran L., Mereghetti S., Götz D., et al., 2005 A&A 432, 467

[37] Mereghetti S., Götz D., Andersen M. I., et al., 2005 A&A 433, 113

[38] Filliatre P., D'Avanzo P., Covino S., et al., 2005, A&A 438, 793